JJEE
Volume 7, Number 2, June 2021
Pages 108-129
Jordan Journal of Electrical Engineering
ISSN (Print): 2409-9600, ISSN (Online): 2409-9619

Functional Electrical Stimulation Assisted Cycling Exercise Optimized By Multi-Objective Genetic Algorithm

Shwan Ch. Abdulla*

Electrical Engineering Department, College of Engineering, University of Sulaimani, Sulaimani, Iraq
E-mail: shwan.abdullah@univsul.edu.iq

Received: October 22, 2020 *Revised: December 25, 2020* *Accepted: January 5, 2021*

***Abstract*—** Cycling exercise - based on functional electrical stimulation (FES) for disabled individuals - is achieved by stimulating single muscle group, the quadriceps, with the help of a new assist mechanism represented by a solid disc flywheel equipped with an electrical clutch. Fuzzy logic based closed-loop control method is implemented to obtain a stable cycling cadence by i) controlling the stimulation intensity on the muscle and ii) managing the engagement of the flywheel mechanism. To achieve better results, several crank positions - with different gear ratios between the crank and the flywheel - are tested and analyzed. To obtain the optimal design parameters, a multi-objective genetic algorithm (MOGA) approach is adopted towards maximizing the cycling efficiency and minimizing the cadence error. A comparison with the results reported in the literature reveals the superiority of the proposed design to limit the cadence error to ±5 rpm for 35 rpm desired speed. Moreover, the results demonstrate that the designed control approach with the proposed assist mechanism is robust to changes in muscle force due to muscle fatigue. Additionally, the introduced control approach with the new assist mechanism is promoting bounded tracking of the desired speed and prolonging FES-cycling training by stimulating the quadriceps muscle group only.

***Keywords*—** Cycling aid mechanism; Functional electrical stimulation; Cadence control; Multi-objective genetic algorithm; Fuzzy control.

1. INTRODUCTION

Functional electrical stimulation (FES) has been applied to re-energize paralytic muscles and restore voluntary functions [1, 2]. FES has shown many psychological and physiological advantages for people who have suffered from spinal cord injuries (SCI). Compared to other types of exercise, cycling has the advantage that the force imposed on the pedal is transformed into motion with high efficiency [3]. The valuable effects of FES-cycling have been observed through the increase in muscle strength, the improvement of blood circulation, reduction in cardiovascular diseases and improvement in cardiopulmonary function [4, 5].

Most FES systems operate in open-loop mode at which the stimulation density is determined heuristically [6]. Since the physiological characteristics of human body vary among individuals and may change by long exercise, fixed stimulation parameters (as in the open-loop approach) need re-tuning from time to time and differ from one individual to another. Also, open-loop approaches can't cope with muscle fatigue or unforeseen mechanical problems [7]. Thus, different closed-loop approaches have been introduced to solve the above problems [8 - 10]. However, muscle fatigue, which accelerates the termination of the exercise, may appear after the use of inappropriate closed-loop control approach due to increased or successive stimulation of the muscle by FES. Also, the robustness of the controller is essential to cope with changes in muscle's physiological parameters - such as muscle fatigue - after long exercise. For these reasons, the choice of a suitable closed-loop control approach is highly important to prevent early termination of the exercise session.

* Corresponding author
Article's DOI: 10.5455/jjee.204-1599462761

In FES-cycling, in addition to improving the control approach, researchers have paid particular attention to improving the exercise outcome, i.e., more comfort, long training and more efficient exercise by means of enhancing the ergometer's design using various aid mechanisms. Some of these researches have used an auxiliary motor connected to the crank - through gears - to aid the leg to pedal in case insufficient force is generated by the muscle [11, 12]. Others have provided hybrid exercise mechanism, by adding an arm-crank, to train the upper and lower limbs of a disabled person and assist the legs when necessary [13]. Other researchers have used a lever arm to optimize the cycling path, i.e., avoiding the dead-spots to produce smoother cycling and enhance the overall efficiency [14, 15].

Besides the employment of an assist mechanism, finding the optimal values of design parameters of both the aid mechanism and the controller is an essential criterion to enhance the FES-cycling performance. The utilized optimization techniques rely on achieving a specific objective, such as prolonging the exercise, increasing the efficiency, increasing the cardiovascular responses and reducing the error in trajectory tracking. Rasmussen et al. [14] optimized the pedaling path and eliminated the cycling dead points by maximizing the activation of the muscle. Gfohler et al. [15] optimized the cycling performance by maximizing the active drive power to improve the efficiency. Huq et al. [16] optimized both the stimulus signal and the variables of the spring used for a lower limb exercise to obtain optimal design parameters of a spring-based orthosis. Other researchers considered the overall energy cost of all muscles involved in the exercise as an objective function to find the metabolically ideal muscle excitation pattern [17]. However, the majority of optimization problems require several objectives to be achieved simultaneously. In such cases, it is difficult to get a single suitable solution for the problem using single-objective optimization method due to the conflicting nature of the objectives.

In FES-cycling exercise, some researchers have stimulated two groups of muscles: extensor muscles such as the quadriceps, and flexor muscles - such as the hamstring - to provide extension and flexion action [13, 18]. Others stimulated the gluteus maximus muscle in addition to the hamstring and the quadriceps [15, 19]. To minimize the preparation time, required to specify the optimum positions of the electrodes, optimize the stimulation parameters for each muscle and to provide more attractive exercise for individuals with SCI, Massoud [20] introduced stimulation patterns to achieve FES-cycling exercise by stimulating only one extensor muscle, the quadriceps, with the help of a spring orthosis to replace the hamstring flexion action.

In a previous work of the author, FES-cycling by stimulating the quadriceps muscle with a novel aid mechanism represented by a flywheel equipped with an electrical clutch, has been introduced [21]. As a storage device, the flywheel interlocks with the crank shaft by the clutch to extract the excessive energy in the bike, convert it to kinetic energy and slow down the cycling when necessary. Also, charged with kinetic energy, it interlocks with the crank shaft to release the stored energy into the system, accelerate the movement and assist the leg if necessary. Results of tests - performed with a fatigue monitor - demonstrated that the aid mechanism was effective in prolonging the exercise by slowing down the occurrence of muscle fatigue. Although the employed control strategy was successful in tracking a predetermined knee trajectory of both legs, crank cadence experienced significant inconstancy. Control of cadence is necessary for studies inspecting the medical and

therapeutic progress and monitoring the effects of exercise at a given speed [22]. In FES-cycling, steady cadence is difficult to maintain by stimulating the quadriceps only, i.e., one-direction actuator, due to the immediate changes in crank's angular velocity caused by the effect of cycling dead points.

In this research, it is aimed to utilize the new aid mechanism in FES-cycling with a closed-loop cadence control approach to achieve cycling speed as close as possible to the reference speed by stimulating the quadriceps muscle only. Also, it is further aimed to optimize the variables of the design (i.e., controller parameters, crank position and gear ratio between the crank's shaft and the flywheel) towards minimizing the cadence error and maximizing the efficiency.

In this paper, information about the cycling power and efficiency, the developed humanoid and bicycle model in addition to the muscle model is given. A fuzzy logic based cadence control approach, utilizing a flywheel with electrical clutch mechanism, is introduced. Investigations with different crank positions and gear ratios are presented. Multi-objective genetic algorithm (MOGA) is used to optimize the parameters of the design. The results are presented, analyzed and compared with those reported in the literature.

2. BACKGROUND ABOUT CYCLING POWER AND EFFICIENCY

The power is realized as the total energy expended per time. Also, the power can be interpreted as the rate to perform work since the transfer of energy is used to achieve work. In mechanical systems, the power is computed as the force on an object multiplied by the object's velocity, i.e., the torque on the bicycle's shaft, or crank, multiplied by the shaft's angular velocity as:

$$P_{out} = \frac{dW}{dt} = \tau.\omega \tag{1}$$

where P_{out} is the cycling power output [w], W is the work performed [J], τ is the torque on the crank [N.m] calculated by multiplying the length of crank arm L [m] with the pedaling force F [N] and ω is the crank's angular velocity [rad/s]. The above equation has been used by several researchers to compute the output power of cycling exercise [23, 24].

The metabolic or mechanical efficiency of a human performing an exercise is considered as the accomplished mechanical work divided by the energy expended during the exercise [25]. The gross efficiency can be calculated as:

$$Efficiency = \frac{Work\ Accomplished\ (W)}{Energy\ Expenditure\ (E)}\ x\,100\ = \frac{P_{out}}{E_{rate}}\ x\,100 \tag{2}$$

where P_{out} is the output power [W] and E_{rate} is the rate of energy consumption [W]. In practice, the energy expended throughout the exercise is calculated by measuring the pulmonary oxygen uptake rate (VO2) [26]. In this work, to calculate the energy consumption rate, muscle energy consumption model proposed in [27] is used to calculate the cycling efficiency.

In this research work, the effect of continually engaging/disengaging flywheel, with the crank shaft, on the overall cycling performance is measured by calculating the flywheel's power throughout the time of engagement with the crank. A solid-disc flywheel's kinetic energy can be calculated as:

$$E_k = \frac{1}{2} I\omega^2 \tag{3}$$

$$I = \frac{1}{2} mr^2 \tag{4}$$

where E_k is the flywheel's kinetic energy [J], I is the inertia [kg.m²], ω is the flywheel's angular velocity [rad/s], m is the mass [kg], and r is the radius [m] of the flywheel.

Since the work is defined as a kind of energy transfer, the derivative of flywheel's kinetic energy (E_k) with respect to time can be employed to calculate the flywheel's power [28] as:

$$P_{FLYWHEEL} = \frac{dW}{dt} = \frac{dE_k}{dt} = I.\alpha.\omega \tag{5}$$

where, $P_{FLYWHEEL}$ is the flywheel's power [w], I is the inertia [kg.m²], α is the flywheel's angular acceleration [rad/s²] and ω is the flywheel's angular velocity [rad/s].

3. SYSTEM DESCRIPTION

3.1. Humanoid and Bicycle Model

Dynamic simulation software, Visual Nastran (vN4D), is utilized to develop a humanoid with a bicycle model. The dimensions used to design the humanoid are based on the standard anthropometric data proposed in [29] at which the weight and length of each single body segment are expressed as a fraction of the total weight and height of the body. The data used to develop the humanoid is based on an individual of 70 kg in weight and 1.80 m in height.

The dimensions of a real bicycle ergometer are used to develop a stationary bicycle model using the same computer program. The flywheel (weight: 3.5 kg, height: 0.01 m, radius: 0.2 m) with an electrically activated clutch mechanism is incorporated with the bike at the center of the crank shaft. The electrical clutch is simulated by an on/off constraint between the crank shaft and the flywheel to provide engagement/disengagement of the flywheel with the crank, when necessary, according to a control signal. Fig. 1 shows the developed humanoid-bicycle model with the flywheel mechanism. Further details about the developed bicycle and humanoid model can be obtained from the author's work in [21].

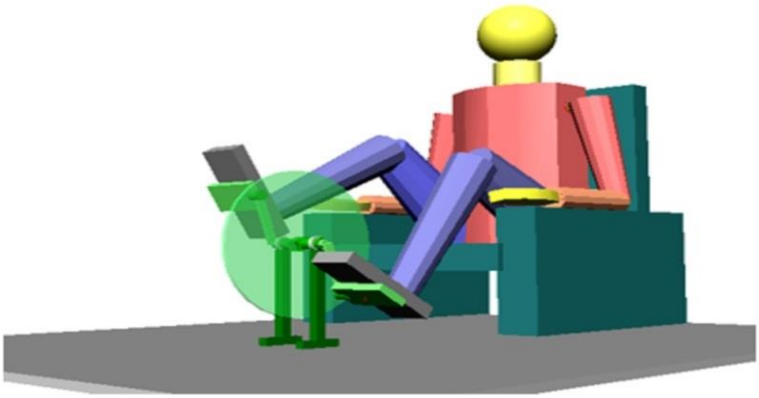

Fig. 1. The developed humanoid-bicycle model with the flywheel mechanism.

3.2. Muscle Model

Researchers have made valuable efforts to study and model the behavior of skeletal muscles that are in charge of the voluntary movement of the body [30-32]. The most accurate muscle models are the ones developed based on the interpretation of the physiological behavior of the muscle.

In this work, to obtain accurate simulation results that are close to reality, a nonlinear physiologically based muscle model proposed in [33-35] is used. The model consists of three essential parts: muscle activation, contraction and segmental dynamics of the body. The activation part identifies the excitation required by the muscle to generate force. It is introduced as a relationship between the frequency and the pulse width of the impulse, including the impact of muscle fatigue, through the fitness function, as well as the calcium dynamics. The following set of functions represents the muscle activation part of the implemented muscle model.

$$a_r(d) = c_1\{(d-d_{\text{thr}})\arctan[k_{\text{thr}}(d-d_{\text{thr}})] \quad -(d-d_{\text{sat}})\arctan[k_{\text{sat}}(d-d_{\text{sat}})]\}+c_2 \tag{6}$$

$$a_f(f) = \frac{(\alpha f)^2}{1+(\alpha f)^2} \tag{7}$$

$$a_{cal}(s) = \left(\frac{1}{\tau_{ca}s+1}\right)\left(\frac{1}{\tau_{ca}s+1}\right)a_{rf}(s) \tag{8}$$

$$\frac{dfit}{dt} = \frac{(fit_{\min}-fit)a_{cal}\lambda(f)}{T_{\text{fat}}} + \frac{(1-fit)(1-a_{cal}\lambda(f))}{T_{\text{rec}}} \tag{9}$$

$$\lambda(f) = 1-\beta+\beta\left(\frac{f}{100}\right)^2 \text{ for } f<100\text{Hz} \tag{10}$$

$$a_{fat}(t) = a_{cal}(t)\ fit(t) \tag{11}$$

where a_r is the recruitment level, d is the pulse width, d_{sat} and d_{thr} represent the saturation and threshold pulse width respectively, c_1, c_2, k_{thr} and k_{sat} are recruitment curve constants, f is stimulation frequency, $a_f(f)$ is the normalized amount of activation, α is a shape factor, a_{cal} is the calcium dynamics, τ_{ca} is a time constant, a_{rf} is the product of recruitment level with amount of activation, fit is muscle fitness, $fit_{\min}$ represents the minimum fitness, T_{fat} is fatigue time, T_{rec} is recovery time, $\lambda(f)$ is a function to consider the relationship between muscle fatigue and stimulus frequency, β is a shape factor, and a_{fat} is muscle fatigue activation.

The muscle contraction part characterizes the force-velocity and force-length properties to represent the force generating feature of the muscle. The following set of functions represents the muscle activation part of the implemented muscle model.

$$f_{\text{fl}} = \exp\left[-\left(\frac{\bar{l}-1}{\varepsilon}\right)^2\right] \tag{12}$$

$$l_i = C_i + \sum_j \int_{\varphi_j} ma_{ij}(\varphi_j)\,d\varphi_j \tag{13}$$

$$f_{\text{fv}} = 0.54\arctan(5.69\bar{v} + 0.51) + 0.745 \quad (14)$$

$$v_i = \sum_j \dot{\varphi}_j \, ma_{ij}(\varphi_j) \quad (15)$$

where f_{fl} is the force-length relation, $\bar{l}$ is the normalized length regarding to the optimal length of muscle (l_{opt}), ε is a shape factor, l_i is the muscle length of group i, ma_{ij} represents the moment of muscle group, i, around joint j, φ_j is the joint position of the muscle, C_i is integration constant, f_{fv} is the force-velocity relation, $\bar{v} = v / |v_m|$ is the normalized velocity regarding to muscle's maximum constriction velocity, v_m, v_i is the muscle velocity of muscle group i, and both $v = dl/dt$ and $v < 0$ for muscle contraction, $\dot{\varphi}_j$ is the muscle joint's angular velocity.

The product of Eqs. (12) to (15) results in the value of muscle force. To produce the active moment of a joint, the joint's moment arm is multiplied by the muscle force. The moment arm functions used are described as:

$$ma_{rf\_H} = 0.025\varphi_H^2 + 0.41\varphi_H - 0.040 \quad (16)$$

$$ma_{rf\_K} = -0.058\exp(-2.0\varphi_K^2)\sin\varphi_K - 0.0284 \quad (17)$$

$$ma_{vs\_K} = -0.070\exp(-2.0\varphi_K^2)\sin\varphi_K - 0.0250 \quad (18)$$

The passive and active moments of the muscle about the joints are considered to describe the segmental dynamics of the body. Considering the effect of adjacent joints on the muscle, double exponential equations are employed to describe the passive elastic properties [36], while a linear damping function is used to characterize the passive viscous property of a muscle [28]. The parameters used for the muscle model implemented in this research are listed in Table 1. For more information, this muscle model is explained in details in [28].

4. CONTROL STRATEGY

The main target in this research work is to obtain prolonged and efficient FES-cycling exercise for paraplegics at a specific cycling speed, i.e., cadence by stimulating the quadriceps muscle. Closed-loop control strategies can be employed to adjust the intensity of the applied signal on the muscle, manage the strength of the force produced by the muscle and maintain the desired leg movement. In addition, by altering the signal's pulse width, the strength of stimulation can be controlled. In this research, the pulse width of the stimulus is kept variable to be regulated by the controller while the frequency of the stimulus is fixed to 33 Hz. A reference cycling speed of 35 rpm is selected as it is the speed generally used in rehabilitation centers [18]. The actual cadence - acquired by a sensor at the crank shaft - is compared with the required reference cadence and the resulting error is fed to the controller to regulate the pulse width consequently.

The quadriceps muscle is activated to produce knee extension that is necessary to obtain forward movement in cycling. Also, to regulate the cycling speed, it is possible to stimulate the quadriceps, at some periods, to produce knee extension and slow down the motion [20]. This approach leads to stimulating the muscle twice per cycle, accelerating the occurrence of muscle fatigue and terminating the exercise [21].

Table 1. Parameters used for the quadriceps muscle model.

Parameter	Rectus Femoris	Vasti
c_1	0.00091	0.00091
c_2	0.4731	0.4731
d_{thr}	122	122
d_{sat}	487	487
k_{thr}	122	122
k_{sat}	487	487
α	0.1	0.1
f	33	33
τ_{ca}	0.03	0.04
$fit_{\min}$	0	0
T_{fat}	18	18
T_{rec}	30	30
β	0.6	0.6
T_{del}	0.025	0.025
l_{opt}	0.086	0.086
ε	0.4	0.45
c_i	0.11	0.04
v_m	0.51	0.48
F_{Max}	450	2340

In this research, the quadriceps muscle of each leg is stimulated once per cycle with the assist of electrically activated clutch/flywheel mechanism, previously introduced by the author of [21]. This mechanism is used to achieve better cadence control by providing appropriate resistance and assistance to the motion when required. As a storage device, the flywheel captures the surplus energy in the bicycle and stores it as kinetic energy when it engages with the crank, hence slowing down the movement. Also, charged with kinetic energy, the flywheel engages with the crank shaft to discharge the stored energy into the system and accelerate the motion. The process of flywheel's engagement/disengagement with/from the crank is performed by means of the electrical clutch.

To regulate the stimulation intensity on the muscle, fuzzy-logic controller (FLC) is used as demonstrated in Fig. 2. The stimulation phases representing the periods are determined according to the crank's angle, at which the controller is allowed to pass its signal to the muscle. Right and left muscle model blocks represent the muscle of right and left legs. Each muscle receives the stimulus of a variable pulse width, according to pre-defined stimulation phases, and produce force supplied to the knee joint of the humanoid-bicycle model to move the leg.

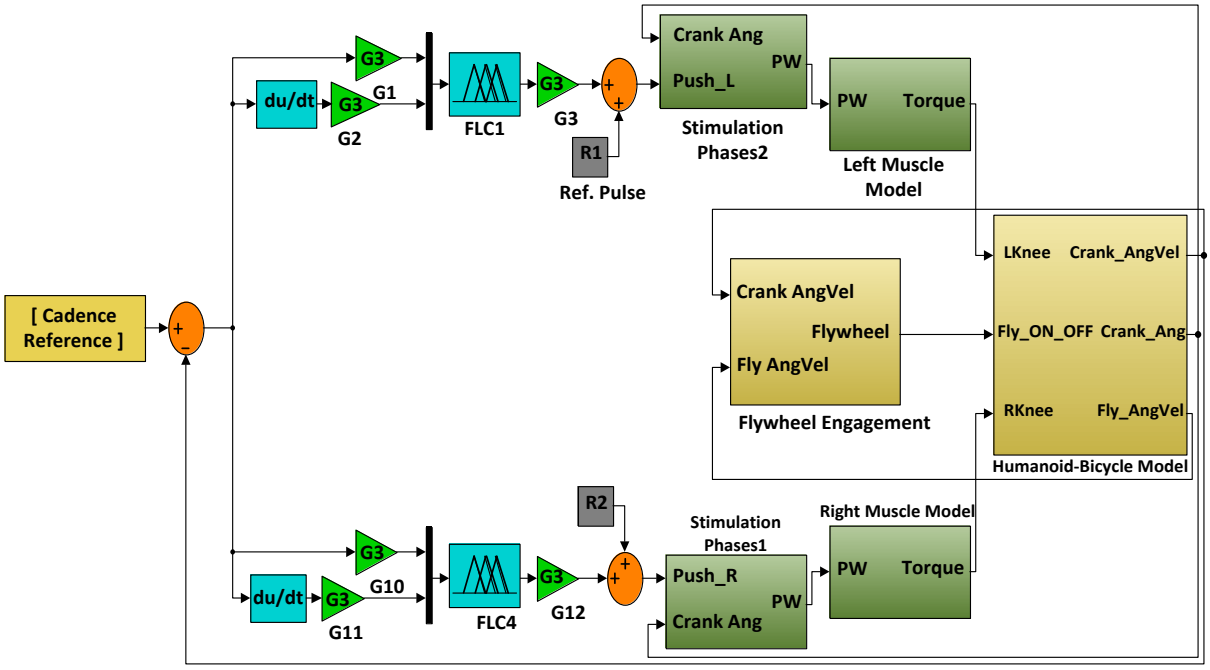

Fig. 2. Block diagram of the FLC controller.

The FLC used is a Mamdani type of double inputs and single output. The output of the FLC specifies the pulse width of the stimulus that is applied on the muscle, while the two inputs indicate the error and derivative of error. Before the fuzzification process, the inputs of the FLC are normalized by a scaling factor. The fuzzification process is performed by a fuzzy set that consists of five Gaussian functions with 50% overlapping. For defuzzification process, center of area(CoA) method is used to convert the fuzzy output to crisp values. A scaling factor is then used to scale the FLC's output. A PD-like fuzzy rule base, of standard 25 rules, is utilized for each controller.

The engagement/disengagement decision of the flywheel is based on the angular velocity of the crank shaft and the flywheel. If the crank shaft rotates faster than the flywheel (i.e., the flywheel can retard the movement) and – simultaneously - if the crank's speed exceeds the reference speed (i.e., the system has excessive energy) the flywheel engages with the crank shaft to absorb the excessive energy and slow down the motion. However, if the crank is slower than the flywheel (i.e. the flywheel is capable of providing assistance) and if - at the same time - the crank's speed is lower than the desired speed, then the flywheel should engage with the crank shaft to release its kinetic energy and accelerate the motion. To control the flywheel engagement process, one Sugeno type FLC - of dual inputs and single output - is used as in Fig. 3.

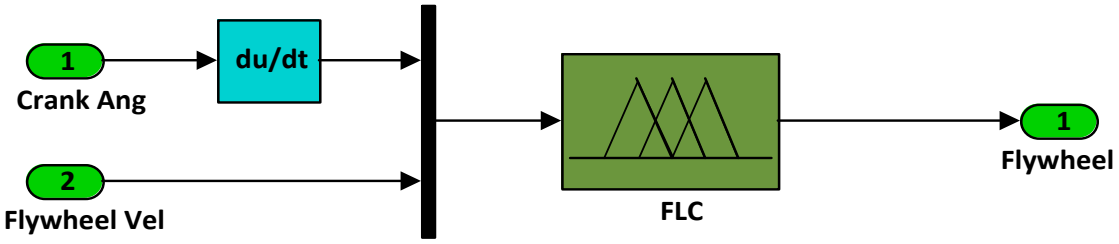

Fig. 3. FLC used to control the flywheel engagement process.

A set of four variables are used to fuzzify the inputs of the FLC. Modified Gaussian membership functions are used to define these variables, namely VeryFast, Fast, Slow and VerySlow, as depicted in Fig. 4. Weighted average defuzzification method is used to change the output - produced by the executed fuzzy rules - to zero or one. Table 2 shows the fuzzy rule base that is used in this controller.

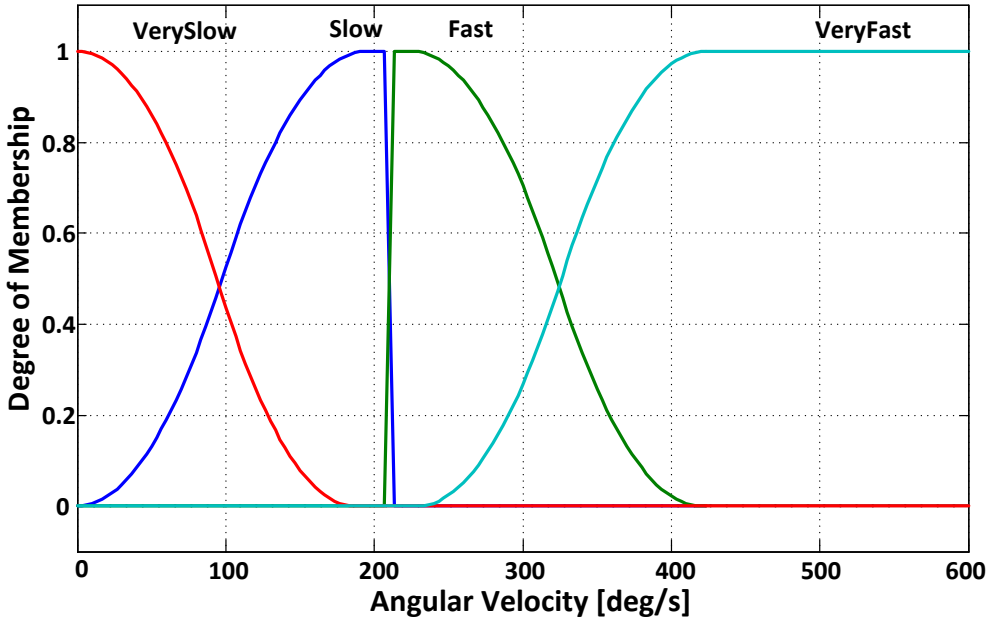

Fig. 4. Modified Gaussian membership functions for the flywheel FLC.

Table 2. Fuzzy rules used for the flywheel FLC.

Crank velocity / Fly velocity	Very Slow	Slow	Fast	Very Fast
Very Slow	*Off*	*Off*	*On*	*On*
Slow	*On*	*Off*	*On*	*On*
Fast	*On*	*On*	*Off*	*On*
Very Fast	*On*	*On*	*Off*	*Off*

The results of the introduced control approach are shown in Figs. 5-7. Although the tracking error is initially large, as in Fig. 5, the control approach with the assist of flywheel mechanism was effective in restricting the variation in cadence by supplying/absorbing energy to/from the crank when required as shown in Fig. 6. The reason behind the initial large tracking error is that the flywheel engagement is activated after the initial two seconds - as shown in Fig. 7 - to visualize the impact of the mechanism in decreasing the cadence error.

In spite of the encouraging results, the cadence error is still large. Further improvement is required by optimizing the controller parameters, the stimulation phases, the crank position as well as the gear ratio between the crank shaft and the flywheel.

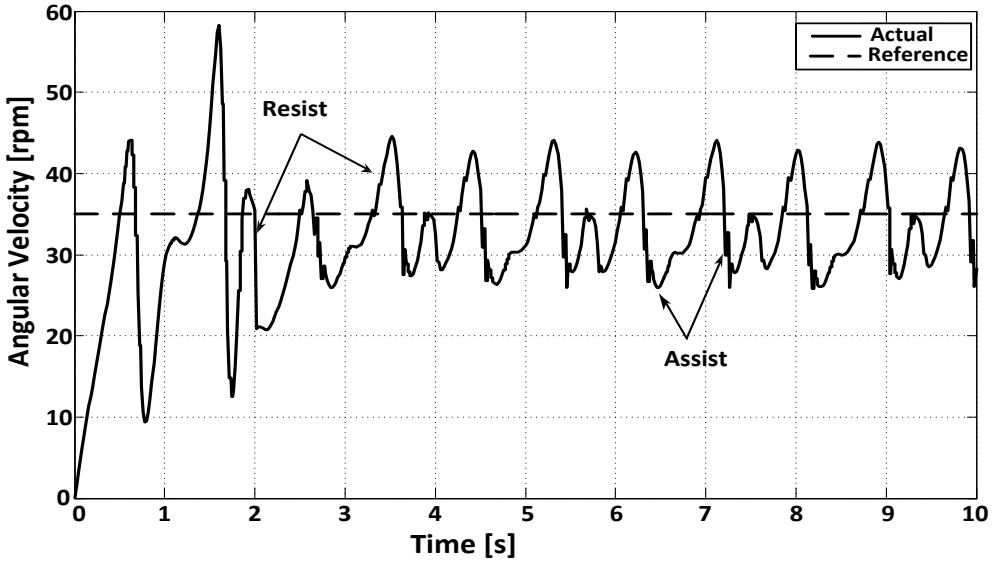

Fig. 5. Angular velocity of the crank tracking a reference cadence.

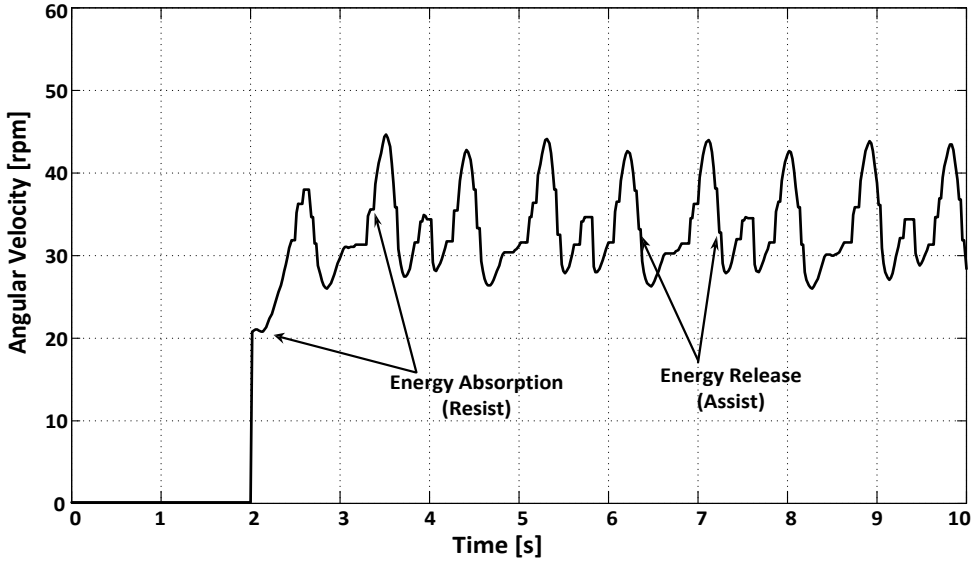

Fig. 6. The flywheel's angular velocity.

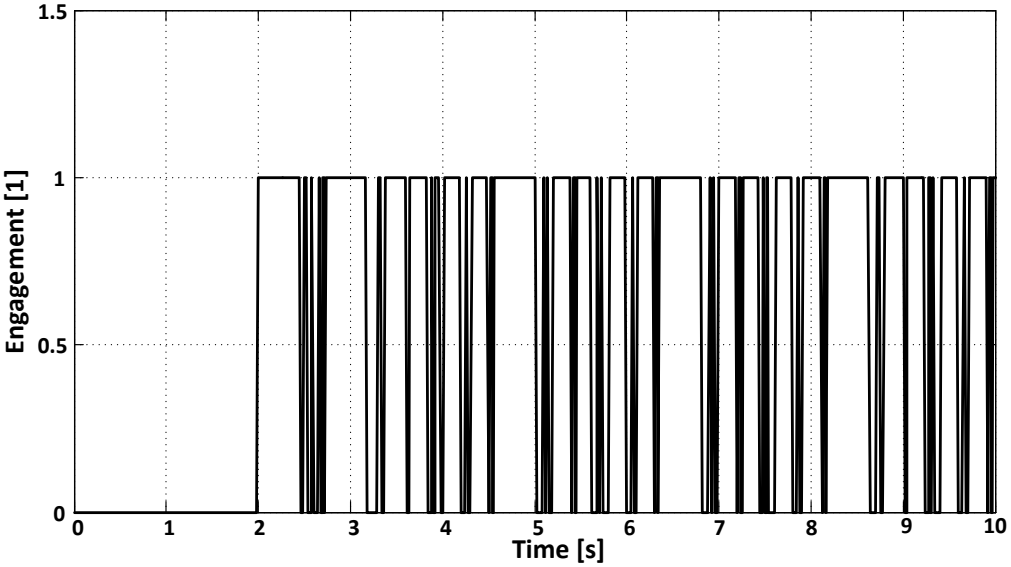

Fig. 7. The engagement periods of the flywheel with the crank.

5. OPTIMIZATION OF DESIGN PARAMETERS

5.1. Crank Position

In the previous section, the center of the crank was at the same vertical point of the hip and at horizontal distance of 0.75 m from the hip. In this section, the objective is to explore the best location of the crank in respect with hip joint, to obtain the maximal benefits from the exercise by means of minimizing the stimulation intensity on the muscle as well as the error in cycling cadence.

To find the best location of the crank, 25 different positions were examined and analyzed. These positions are carried out as 5 different vertical positions with 5 different horizontal positions for each vertical position. The vertical positions ranged between -0.1 m and 0.1 m with increments of 0.05 m. While the horizontal positions (i.e., the span between the hip joint and the center of the crank) ranged between 0.6 m and 0.8 m, with 0.05 m increments. As illustrated in Fig. 8, the 25 different positions are demonstrated as an array of 25 dot points. Since the design dimensions cannot be modified automatically - due to restrictions of Visual Nastran software used to design the humanoid/bicycle model - each position was tested separately.

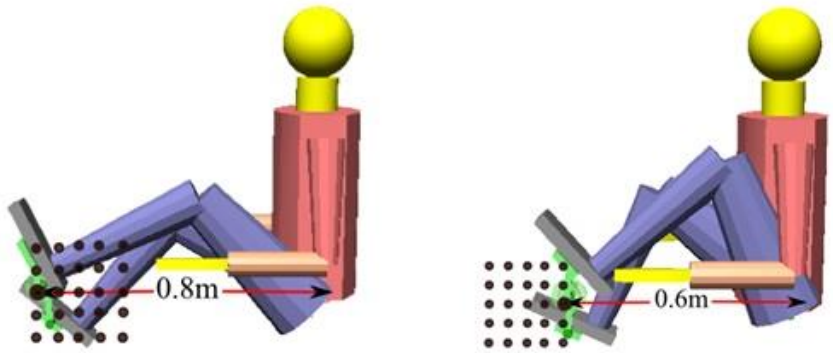

Fig. 8. Illustration of the tested 25 different positions of the crank with respect to the hip.

For the currently used bicycle dimensions, it is observed that at the 0.8 m horizontal position, the cycling wasn't achievable for all the 5 vertical positions. The reason beyond this is the large interval between the crank location and the hip when using a 0.14 m crank arm; thus the person won't be able to pedal. The results of the remaining 20 crank positions are recorded - as shown in Figs. 9 and 10 - and the total performance is analyzed.

The main target of the tuning carried out at each position is to obtain the minimal cadence error. The best percentage in cadence error - recorded at each crank position - is presented in Fig. 9. It is evident from the figure that the error was large at position 0.6 m. This is because the cyclic movement was very hard to control at this position. The reasoning beyond this is that the trunk and the thigh of one leg become too close to each other and, consequently, produce resistance to other leg's motion. Further, the error was considerably high at position 0.75 m. This is because the thigh was nearly extended at this position and the impact of the dead points predominated and caused the large error in cadence. At positions 0.7 m and 0.65 m the error was around 13%, which is nearly similar for all vertical positions. This is because the distance between these positions and the hip were moderate and, consequently, led to much easier control of pedaling movement.

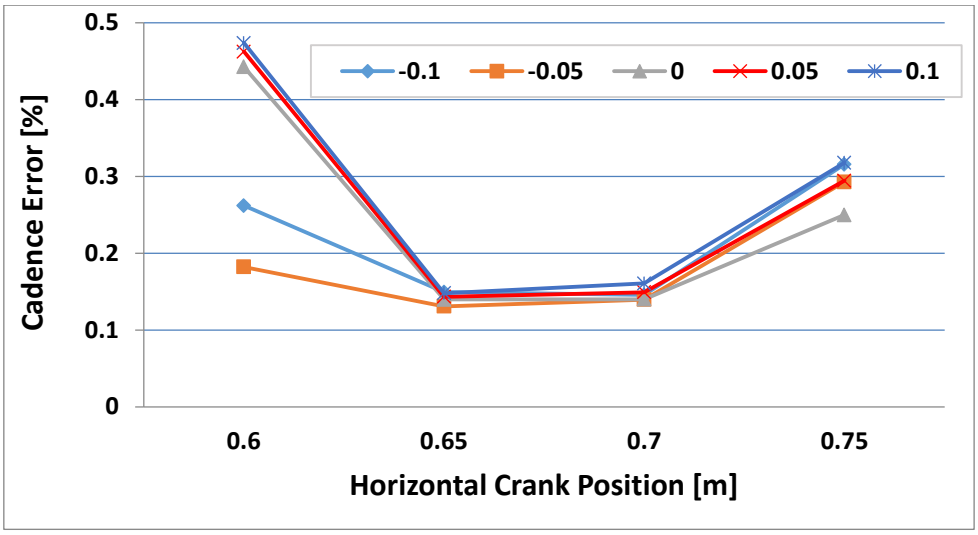

Fig. 9. Cadence percentage error at different horizontal and vertical positions of the crank.

Fig. 10 displays the average efficiency of cycling for various positions of the crank. It is evident that at positions 0.7 m and 0.65 m, the average efficiency was low as compared with positions 0.75 m and 0.6 m.

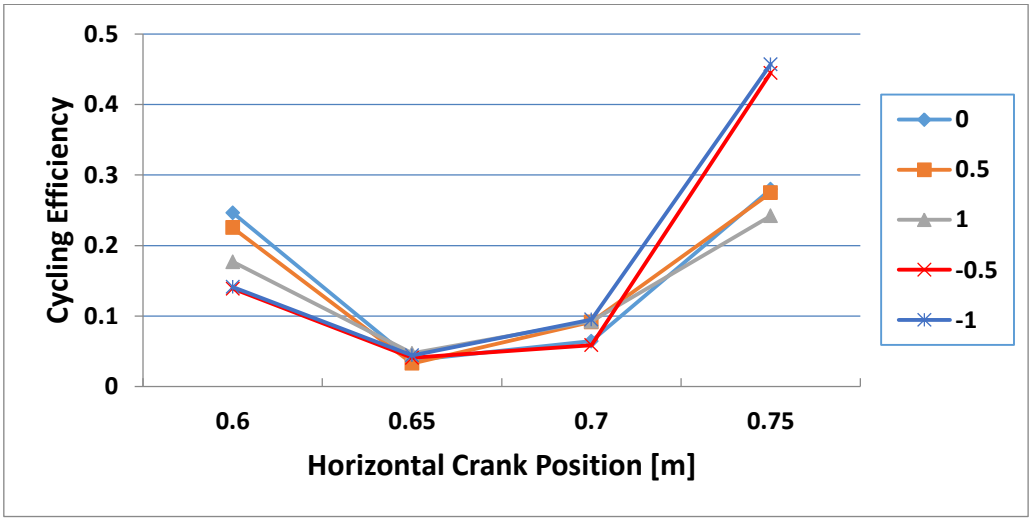

Fig. 10. Average cycling efficiency for different horizontal and vertical positions of the crank.

The least percentage error in cycling cadence was limited at positions (0.65, -0.5), (0.65, 0), (0.7, -0.5) and (0.7, 0). However, at position (0.7, 0) an efficiency of 6.44% is achieved which is higher than that at crank position (0.65, -0.5) of 4.08%. In addition, the average stimulation of 203.05 μs at position (0.65, -0.5) was higher than that of 183.41 μs at position (0.7, 0). It was thus preferred to select position (0.7, 0) as the optimal crank position for its relatively high efficiency, low stimulation intensity and reasonable error values.

5.2. Gear Ratio with Optimal Crank Position

Transmission systems usually use gears to acquire mechanical advantages, i.e., changes in torque and speed, through a gear between the device and its load [37]. The gear ratio R is defined as:

$$R = \frac{\omega_A}{\omega_B} = \frac{N_B}{N_A} = \frac{\tau_B}{\tau_A} = \frac{r_B}{r_A} \quad (19)$$

where ω [rad/s] represents the angular velocity, τ is the torque, N is the number of gear teeth, r is the gear radius, A and B are the gears of driver and driven machines, respectively.

Our main objective here is to decrease the cycling cadence error and improve the performance of FES-cycling by using an appropriate gear ratio - between the flywheel and the crank shaft - while the crank is at position (0.7, 0), i.e., horizontally 0.7 m and vertically 0.0 m distant from the hip joint. In the introduced flywheel aid mechanism, the gear ratio has a significant role in altering the amount of assistance/resistance produced by the flywheel. For this reason - to identify the optimal gear ratio of the mechanism - 17 different ratios varying from 0.33 to 3.0 were examined. To test various gear ratios, a gear constraint is set up between the crank shaft and the flywheel in the bicycle model. Some of the tested gear ratios are greater than one (when the crank's gear is smaller in diameter and also in number of teeth than the flywheel's gear), while other ratios are smaller than one (when the crank's gear is greater than the flywheel's gear). When engagement takes place with a gear ratio larger than one, the flywheel will rotate half the crank speed. On the other hand, with a gear ratio smaller than one, the flywheel will rotate twice the crank speed.

The control strategy employed in this section is similar to that in discussed section 4. The sole difference is the addition of an input scaling factor for the flywheel mechanism, to scale up or down the flywheel's angular velocity in accordance with the gear ratio. This is essential for the mechanism to provide proper engagement/disengagement of the flywheel when necessary. The value of the flywheel angular velocity scaling factor (FAVSF) used in this section is the same as the value of the utilized gear ratio.

The results of this section, recorded for 10 s, are shown in Figs. 11-13. The cycling percentage error dropped to less than 11% at gear ratios between 0.67-0.83. It is noticed that at ratios smaller than 0.60, the error increased because the amount of damping - caused by these ratios - was high as the flywheel speed increases with the reduction of the ratio, and hence the energy absorbed (i.e., resistance) from the crank. On the other side, at gear ratios bigger than one, the error was also large because with these gear ratios the flywheel absorbed small amount of crank energy when resist action was required, hence the flywheel was unable to provide either sufficient resistance or assistance to the motion. Fig. 12 shows the flywheel's average power at periods of engagement. The flywheel's average power was positive with gear ratios lower than one. This shows that the resistive role of the flywheel in average is more than being assistive, due to the absorption of crank's energy. Therefore, it burdens the system with slight load. This explains the drop in efficiency at these gear ratios as exhibited in Fig. 13. It was noticed that with gear ratios larger than one, the flywheel power was almost negative. This means that the flywheel had discharged its energy into the system and on average had assistive role more than resistive. However, as the flywheel's energy - absorbed and released with these gear ratios - was small, it had no remarkable effect on the system.

The least possible error in cycling cadence was limited between 0.67-0.83 gear ratios. However, the cycling efficiency and the average stimulation intensity were 6.3% and 151.70 μs, respectively, at gear ratio 0.67. With gear ratio equal to 0.83, the cycling efficiency was 6.82% whereas the stimulation intensity was 149.11 μs. For these statistics, the 0.83 gear ratio is selected as the optimal gear ratio for crank location (0.7, 0.0).

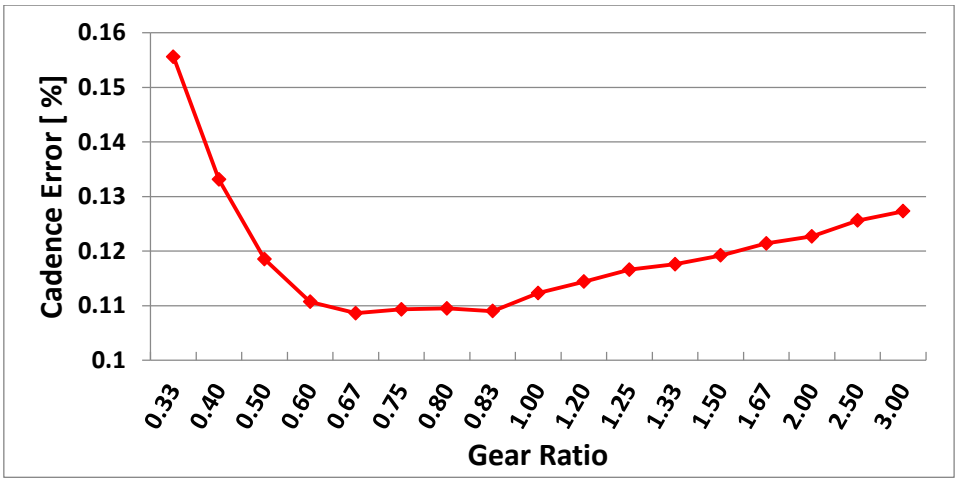

Fig. 11. Percentage error in cadence at different gear ratios.

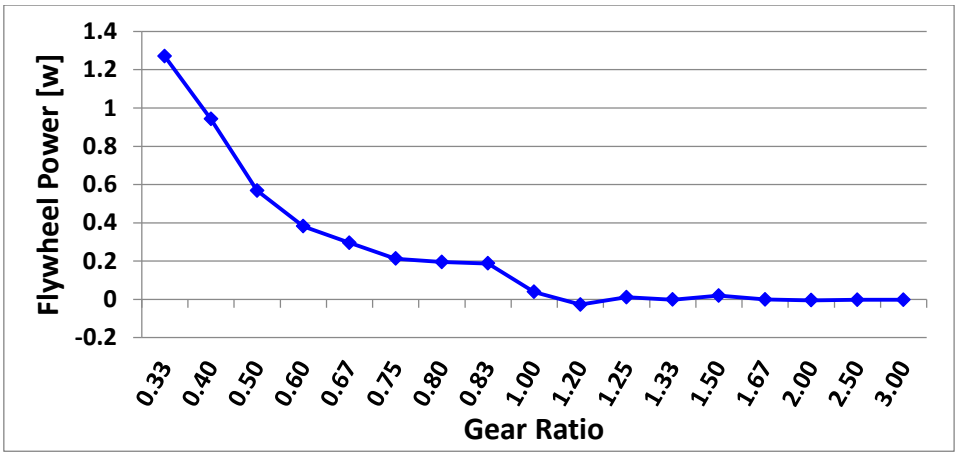

Fig. 12. Flywheel power at different gear ratios.

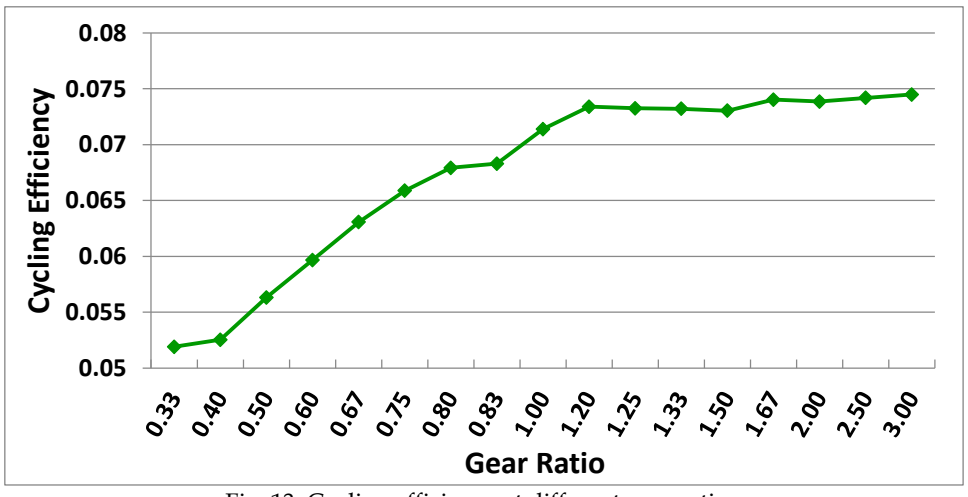

Fig. 13. Cycling efficiency at different gear ratios.

5.3. MOGA to Optimize FES-Cycling Parameters

Multi-objective optimization is a stochastic search algorithm used for issues having multi objective functions to be optimized simultaneously. It has been utilized in many different areas of finance, logistics and engineering [38-41] to discover the optimum solution, as a trade-off of two or more contradicting solutions.

A non-dominated or Pareto optimal solution is the one at which there is no possibility to improve the value or the quality of one objective function without deteriorating the value of others. The main goal is to discover a set of non-dominated solutions and select an optimal solution as a trade-off in meeting different objectives according to the preference of decision makers.

The MOGA, proposed in [42], was one of the earliest methods that utilized the concept of non-dominated optimal set. The MOGA is set by a group of individuals, called population, with a group of operators that alters these individuals. Each of these individuals is supposed as a potential solution to the problem. Initially several individual solutions are randomly created to construct the initial group of population. Each single individual is converted into a binary string, known as a chromosome, to be evaluated. The chromosomes are then developed to form superior solutions to the issue.

In MOGA, after evaluating each chromosome by the objective function and obtaining the initial fitness, ranking based fitness sharing technique is used to estimate new fitness value to be employed for selection purposes towards finding the non-dominated, or Pareto, optimal set of solutions. The ranking of each individual, or chromosome, in the population correlates with the overall number of chromosomes by which it is predominated. To form the next generation, the more fit individuals - depending on their calculated fitness - are chosen for mating and breeding. The characteristics of each selected individual are amended - through crossover and mutation operations - to generate new offspring for the next population. The flow chart of MOGA implemented in this research is presented in Fig. 14.

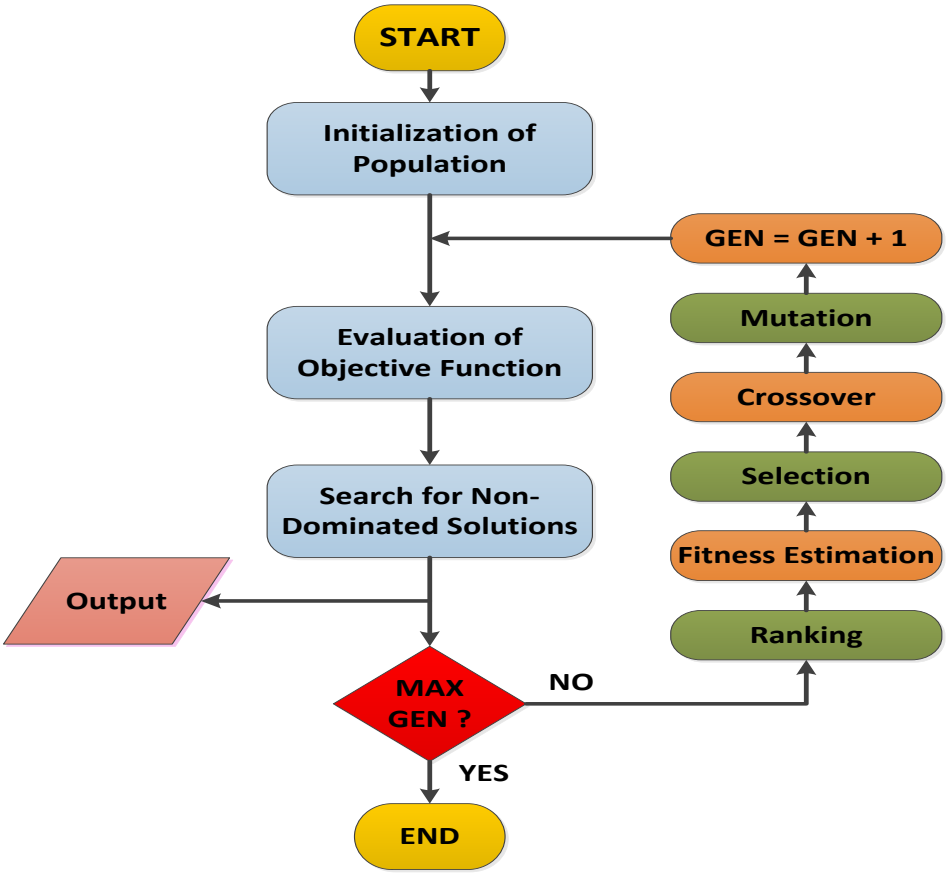

Fig. 14. Flow chart of MOGA process.

The main objective here is to utilize the MOGA to optimize the design variables for maximum cycling efficiency and minimum cadence error simultaneously. There are eleven different parameters in the design to be tuned. These parameters are the two inputs (K1 and K2) and output (K3) scaling factors of the fuzzy logic controller, the reference pulse value (K4), the FAVSF (K5), the minimum (K6) and maximum (K7) saturation values of the FLC output at pushing phase, the start (K8) and the end (K9) of pushing phase as a crank angle, the flywheel's weight (K10) and the flywheel mechanism's activation time (K11).

The algorithm is run for 100 generations with an initial population of 40 individuals. Gray coding is used to encode each one of these eleven parameters by 20 binary strings. The strings then concatenated to shape the ultimate chromosome. The mutation and the crossover operators were specified to 0.01 and 80%, respectively.

In this optimization process, two objective functions are used: i) minimize the cadence percentage error and ii) maximize the cycling efficiency. The two objective equations are given as:

$$ObjectiveFunc.1 = \min\left\{\frac{\sum_{i=1}^{N}(y_{ref} - y_{act})^2}{N.y_{ref}}\right\} \tag{20}$$

$$ObjectiveFunc.2 = \min\{\frac{Muscle\,Power}{Output\,Power}\} = \min\{\frac{1}{Efficiency}\} \tag{21}$$

where y_{act} is the crank's actual angular velocity, y_{ref} is the desired angular velocity, and N is the number of samples.

The Pareto, non-dominated, optimal set of solutions achieved by MOGA at the end of 100 iterations is depicted in Fig. 15. It is evident that the optimization algorithm generated a rich set of Pareto solutions as a negotiation between the two mentioned objectives. Additionally, it is noticeable from Fig. 15 that solutions of high percentage error in cadence are accompanied with high efficiency values.

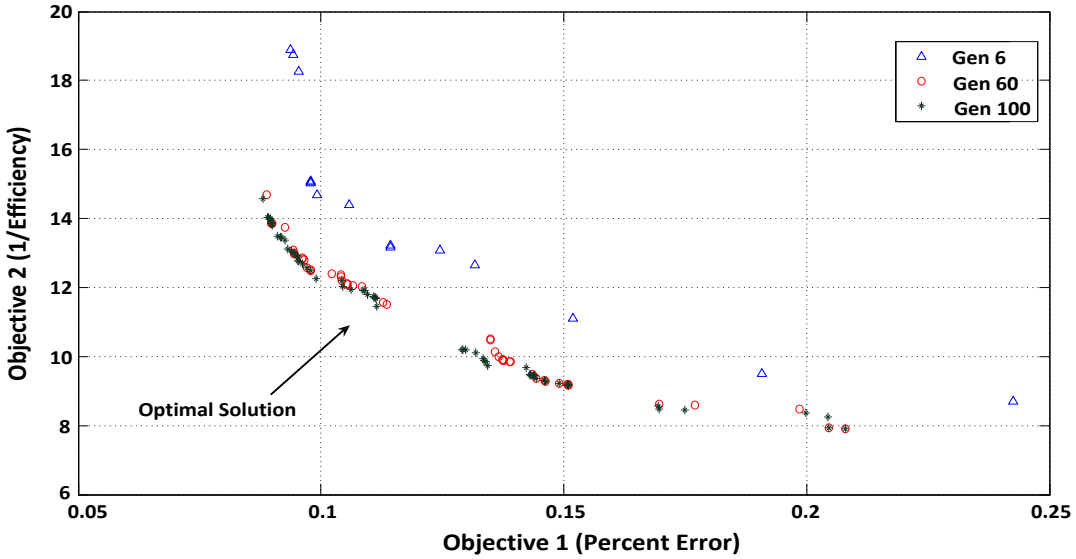

Fig. 15. The optimal solution selected after 100 iteration using MOGA.

In order to obtain acceptable cycling efficiency and maintain as minimum error in cadence as possible, one of the solutions is selected as the optimal solution. Table 3 shows the optimized values of design variables at the selected optimal solution. Utilizing the optimal solution, the efficiency in cycling - registered for 10 s - is 8.17% while the cadence percentage error is 9.9%.

Table 3. The optimized design parameters achieved by using the optimal solution.

Parameter	K1	K2	K3	K4	K5	K6	K7	K8	K9	K10	K11
Value	0.0139	0.0166	246.2690	212.0339	0.3201	-0.6684	0.6917	9.8227	122.2180	3.5287	1.6429

6. RESULTS EVALUATION AND DISCUSSION

The optimized parameters obtained by using the optimal solution are utilized and examined for 300 s. After the activation of the flywheel aid mechanism took place in 1.6 s, for a 35 rpm cadence reference, the measured cadence ranged between 30-40 rpm for the entire duration of the exercise as presented in Fig. 16. The time fatigue constant (T_{fat}) of the quadriceps model is dropped from 18 to 4 s - as used in the literature [9] - to examine the robustness and the durability of the utilized control approach to rapid muscle fatigue problem. The measured cadence experienced a slight change, but remained bounded within 30-40 rpm as can be observed from Figs. 16 and 17. This demonstrates the robustness of the introduced control approach to effectively deal with possible drops in muscle fitness of the individual during the exercise.

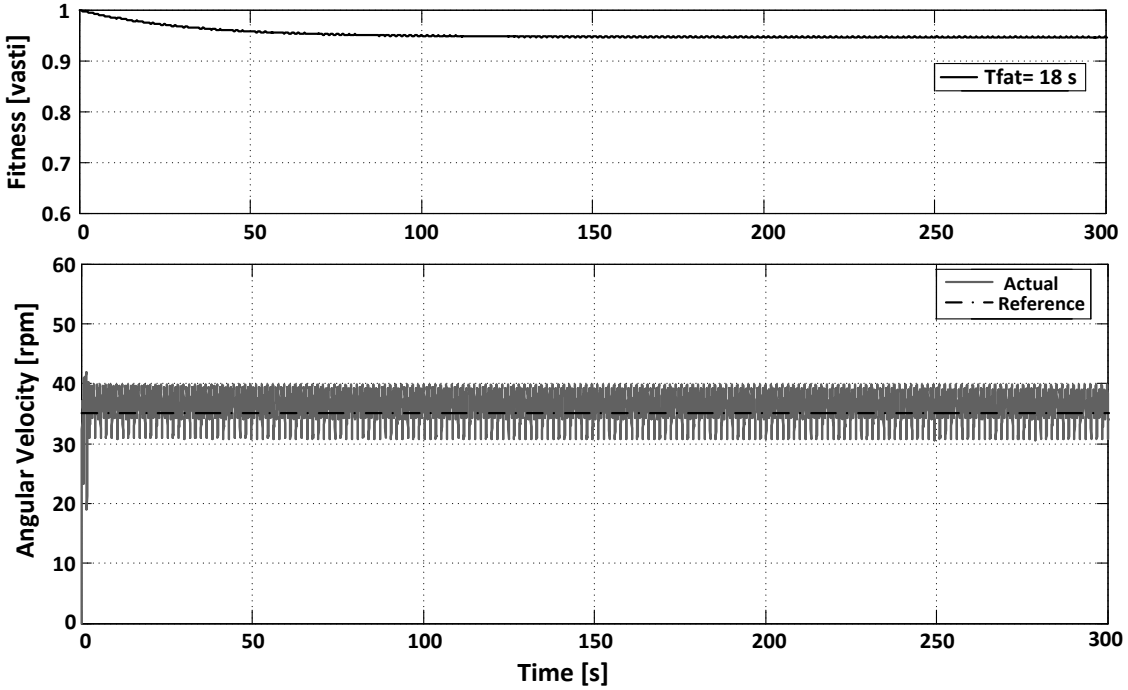

Fig. 16. The recorded angular velocity of the crank with muscle time fatigue constant equal to 18 s.

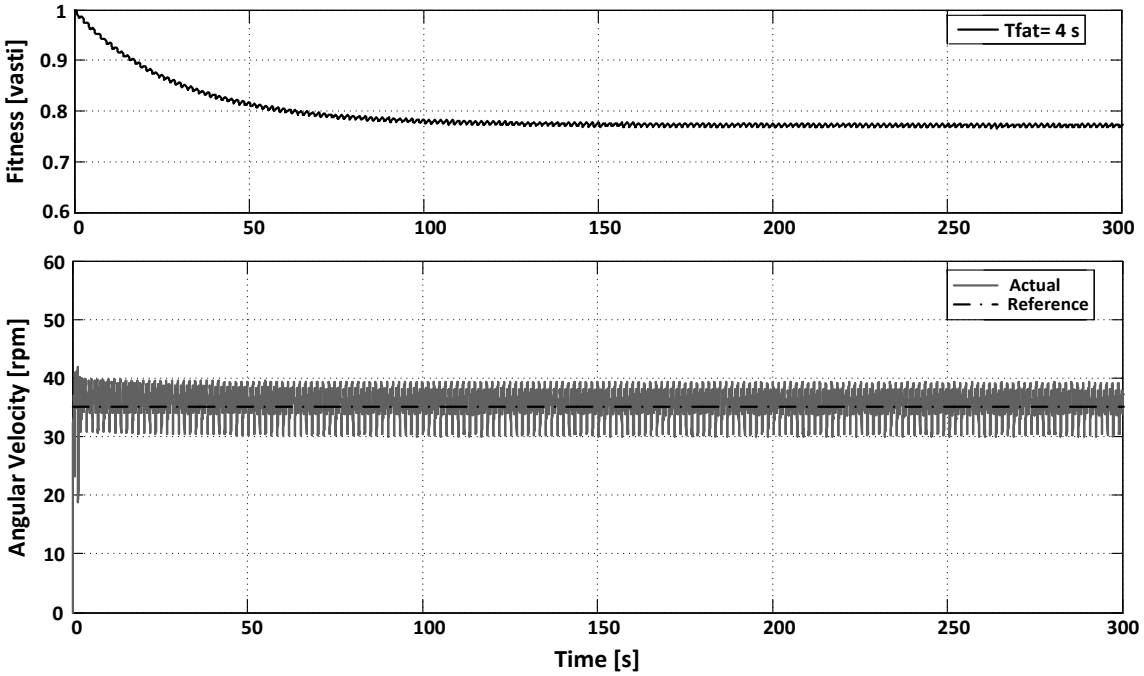

Fig. 17. The recorded angular velocity of the crank with muscle time fatigue constant equal to 4 s.

The design is also tested with different desired speeds frequently used in rehabilitation centers. The obtained lowest and highest speed limits are exhibited in Table 4. It is evident that the cadence error has slightly increased with the increase of the desired speed. Even though, the cadence error is still reasonable for cycling with single muscle.

Table 4. Cycling performance at different speeds.

Desired speed [rpm]	Minimum speed [rpm]	Maximum speed [rpm]
35	30.8	39.9
45	39.1	49.8
55	45.7	59.4

For evaluation purposes, the crank's actual angular velocity, i.e., cycling cadence measured in this research is compared with that achieved in [13] as both studies utilized fuzzy logic control method. In [13], the hamstring together with the quadriceps, i.e., flexor and extensor muscles, have been used with an arm crank assist mechanism. It is evident from Fig. 18(a) that the cadence error - recorded in this work for 35 rpm speed reference - ranged between ±5 rpm by stimulating the quadriceps with the assist of the flywheel mechanism. The cadence achieved in [13] as shown in Fig. 18(b) for a speed reference of 50 rpm has oscillated for more than ±10 rpm. The performance at other desired speeds, as shown in Table 4, is still superior as compared to that reported in [13]. In addition, the cycling efficiency obtained in this work, which is 8.17%, is acceptable as the FES-cycling efficiency ranges between 2% to 14% in disabled individuals [43, 44].

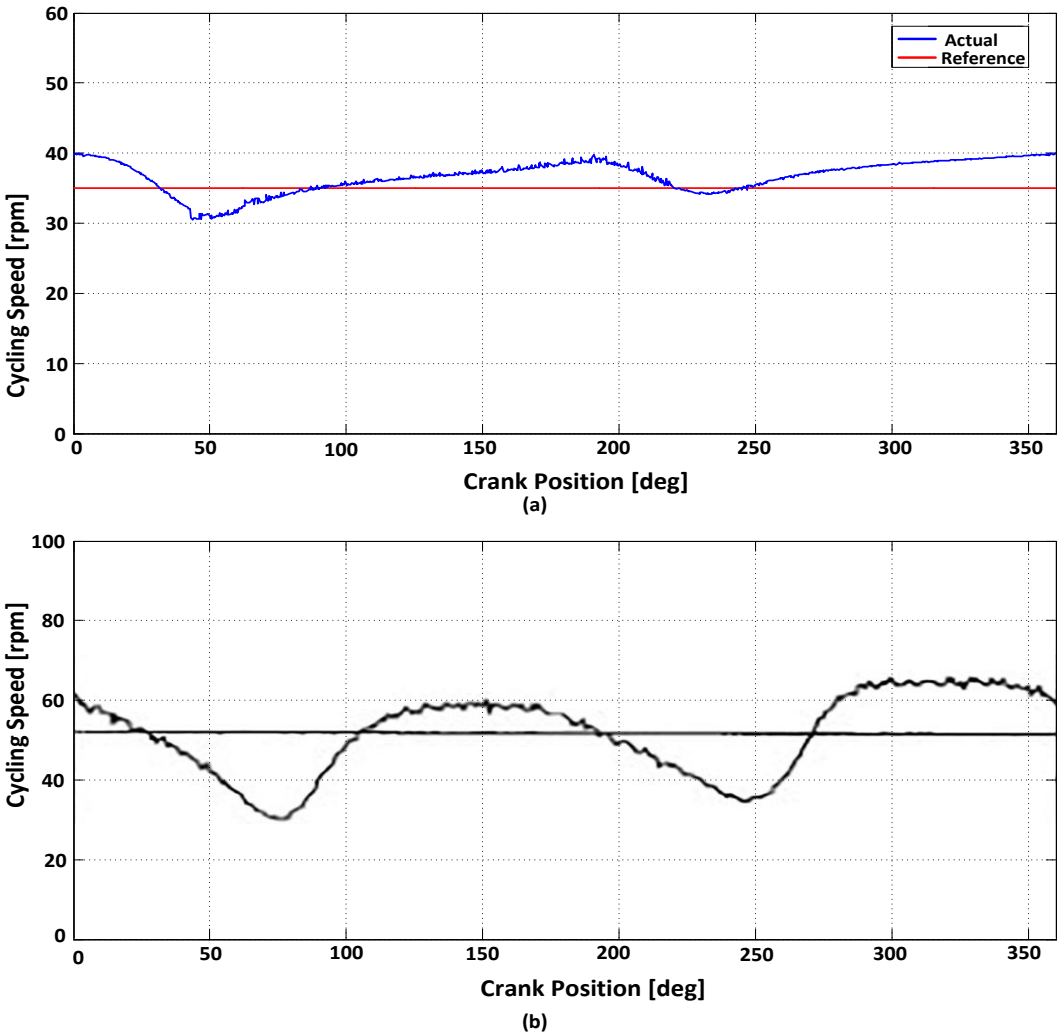

Fig. 18. Cycling cadence utilizing: a) 35 rpm cadence reference (this investigation); b) 50 rpm cadence reference reported in [13].

7. CONCLUSIONS AND FUTURE WORK

A closed-loop cadence control approach - to manage the stimulation intensity on the quadriceps muscle and control the operation of a flywheel mechanism in FES-cycling exercise - has been presented. A solid disc flywheel - as a storage device - has been utilized to provide damping (i.e., resistance) effect on the speed by absorbing the surplus energy in the bicycle and storing it as kinetic energy when necessary. Also, when the flywheel is charged with kinetic energy, it interlocks with the crank shaft to accelerate the motion and assist the legs when required. The engagement/disengagement is performed by an electrical clutch mechanism. The optimal gears between the flywheel and the crank shaft, and the optimal interspace between the hip joint and the crank have been specified. Using MOGA, the optimal design parameters for best performance, in terms of maximum efficiency and minimum cadence error, have been specified and tested using dynamic simulation software.

The obtained results showed that the introduced control approach - together with the flywheel aid mechanism - can produce cycling exercise of high efficiency and bounded cadence error with robustness to premature muscle fatigue related problems. This leads to a conclusion that the introduced approach is promoting efficient and prolonged FES-cycling exercise.

A variable gear mechanism to produce different gear ratios between the crank and the flywheel can be investigated to provide assistance to different individuals with different cycling speeds. Also, a prototype cycling ergometer with the proposed assist mechanism can be built, tested and validated in subsequent stages. However, safety issues, i.e., protection circuit against spasticity or unexpected mechanical problems, need to be considered before clinical usage.

REFERENCES

[1] S. Sabut, C. Sikdar, R. Mondal, R. Kumar, M. Mahadevappa, "Restoration of gait and motor recovery by functional electrical stimulation therapy in persons with stroke," *Disability and Rehabilitation*, vol. 32, no. 19, pp. 1594-1603, 2010.

[2] T. Thrasher, H. Flett, M. Popovic, "Gait training regimen for incomplete spinal cord injury using functional electrical stimulation," *Spinal Cord*, vol. 44, no. 6, pp. 357-361, 2005.

[3] M. Gföhler, M. Loicht, P. Lugner, "Exercise tricycle for paraplegics," *Medical and Biological Engineering and Computing*, vol. 36, no. 1, pp. 118-121, 1998.

[4] G. Davis, N. Hamzaid, C. Fornusek, "Cardiorespiratory, metabolic, and biomechanical responses during functional electrical stimulation leg exercise: health and fitness benefits," *Artificial Organs*, vol. 32, no. 8, pp. 625-629, 2008.

[5] N. Donaldson, T. Perkins, R. Fitzwater, D. Wood, F. Middleton, "FES cycling may promote recovery of leg function after incomplete spinal cord injury," *Spinal Cord*, vol. 38, no. 11, pp. 680, 2000.

[6] J. Abbas, R. Triolo, "Experimental evaluation of an adaptive feedforward controller for use in functional neuromuscular stimulation systems," *IEEE Transactions on Rehabilitation Engineering*, vol. 5, no. 1, pp. 12-22, 1997.

[7] J. Abbas, H. Chizeck, "Neural network control of functional neuromuscular stimulation systems: computer simulation studies," *IEEE Transactions on Biomedical Engineering*, vol. 42, no. 11, pp. 1117-1127, 1995.

[8] A. Farhoud, A. Erfanian, "Higher-order sliding mode control of leg power in paraplegic FES-cycling," *Annual International Conference of the IEEE Engineering in Medicine and Biology*, pp. 5891-5894, 2010.

[9] C. Kim, G. Eom, K. Hase, G. Khang, G. Tack, J. Yi, J. Jun, "Stimulation pattern-free control of FES cycling: simulation study," *IEEE Transactions on Systems, Man, and Cybernetics, Part C: Applications and Reviews*, vol. 38, no. 1, pp. 125-134, 2008.

[10] S. Jezernik, R. Wassink, T. Keller, "Sliding mode closed-loop control of FES controlling the shank movement," *IEEE Transactions on Biomedical Engineering*, vol. 51, no. 2, pp. 263-272, 2004.

[11] D. Pons, C.Vaughan, G. Jaros, "Cycling device powered by the electrically stimulated muscles of paraplegics," *Medical and Biological Engineering and Computing*, vol. 27, no. 1, pp. 1-7, 1989.

[12] T. Perkins, N. Donaldson, N. Hatcher, I. Swain, D. Wood, "Control of leg-powered paraplegic cycling using stimulation of the lumbo-sacral anterior spinal nerve roots," *IEEE Transactions on Neural Systems and Rehabilitation Engineering*, vol. 10, no. 3, pp. 158-164, 2002.

[13] K. Chen, S. Chen, K. Tsai, J. Chen, N. Yu, M. Huang, "An improved design of home cycling system via functional electrical stimulation for paraplegics," *International Journal of Industrial Ergonomics*, vol. 34, no. 3, pp. 223-235, 2004.

[14] J. Rasmussen, S. Christensen, M. Gföhler, M. Damsgaard, T. Angeli, "Design optimization of a pedaling mechanism for paraplegics," *Structural and Multidisciplinary Optimization,* vol. 26, no. 1-2, pp. 132-138, 2004.

[15] M. Gfohler, T. Angeli, T. Eberharter, P. Lugner, W. Mayr, C. Hofer, "Test bed with force-measuring crank for static and dynamic investigations on cycling by means of functional electrical stimulation," *IEEE Transactions on Neural Systems and Rehabilitation Engineering*, vol. 9, no. 2, pp. 169-180, 2001.

[16] M. Huq, M. Alam, S. Gharooni, M. Tokhi, "Genetic optimization of spring brake orthosis parameters: spring properties," *The 10th Annual Conference on of International Functional Electrical Stimulation Society*, Montreal, Canada, pp. 279-281, 2005.

[17] E. Idsø, T. Johansen, K. Hunt, "Finding the metabolically optimal stimulation pattern for FES-cycling," *9th Annual Conference of the International Functional Electrical Stimulation Society*, Bournemouth, UK, pp. 171-173, 2004.

[18] J. Chen, N. Yu, D. Huang, B. Ann, G. Chang, "Applying fuzzy logic to control cycling movement induced by functional electrical stimulation," *IEEE Transactions on Rehabilitation Engineering*, vol. 5, no. 2, pp. 158-169, 1997.

[19] C. Fornusek, G. Davis, P. Sinclair, B. Milthorpe, "Development of an isokinetic functional electrical stimulation cycle ergometer," *Neuromodulation: Technology at the Neural Interface*, vol. 7, no. 1, pp. 56-64, 2004.

[20] R. Massoud, *Intelligent Control Techniques for Spring-Assisted FES-Cycling*, Ph.D. dissertation submitted to the Department of Automatic Control and System Engineering, The University of Sheffield, United Kingdom, 2007.

[21] S. Abdulla, O. Sayidmarie, M. Tokhi, "Functional electrical stimulation-based cycling assisted by flywheel and electrical clutch mechanism: A feasibility simulation study," *Robotics and Autonomous Systems*, vol. 62, no. 2, pp. 188-199, 2014.

[22] K. Hunt, M. Rothe, T. Schauer, A. Ronchi, N. Negård, "Automatic speed control in FES cycling," *6th Annual Conference of the International Functional Electrical Stimulation Society*, pp. 300-302, 2001.

[23] B. Stone, *Control Strategies for Functional Electrical Stimulation Induced Cycling*," University of Glasgow, 2005.

[24] K. Hunt, B. Stone, N. Negard, T. Schauer, M. Fraser, A. Cathcart, C. Ferrario, S. Ward, S. Grant, "Control strategies for integration of electric motor assist and functional electrical stimulation in paraplegic cycling: utility for exercise testing and mobile cycling," *IEEE Transactions on Neural Systems and Rehabilitation Engineering*, vol. 12, no. 1, pp. 89-101, 2004.

[25] K. Hunt, J. Fang, J. Saengsuwan, M. Grob, M. Lau-bacher, "On the efficiency of FES cycling: a framework and systematic review," *Technology and Health Care*, vol. 20, no. 5, pp. 395-422, 2012.

[26] C. Ferrario, *Functional Electrical Stimulation (FES) Leg Cycling Exercise in Paraplegia: A Pilot Study for the Definition and Assessment of Exercise Testing Protocols and Efficacy of Exercise*, University of Glasgow, 2006.

[27] B. Umberger, K. Gerritsen, P. Martin, "A model of human muscle energy expenditure," *Computer Methods in Biomechanics and Biomedical Engineering*, vol. 6, no. 2, pp. 99-112, 2003.

[28] A. Giambattista, B. Richardson, R. Richardson, *College Physics*, New York, London : McGraw-Hill, 2007.

[29] D. Winter, *Biomechanics and Motor Control of Human Movement*, John Wiley and Sons Inc., 1990.

[30] F. Zajac, "Muscle and tendon: properties, models, scaling, and application to biomechanics and motor control,"*Critical Reviews in Biomedical Engineering*, vol. 17, no. 4, p. 359, 1989.

[31] M. Ferrarin, A. Pedotti, "The relationship between electrical stimulus and joint torque: a dynamic model," *IEEE Transactions on Rehabilitation Engineering*, vol. 8, no. 3, pp. 342-352, 2000.

[32] R. Jailani, M. Tokhi, S. Gharooni, Z. Hussain, "Development of dynamic muscle model with functional electrical stimulation," *Complexity in Engineering*, Rome, Italy, pp. 132-134, 2010.

[33] R. Riener, J. Quintern, "A physiologically based model of muscle activation verified by electrical stimulation," *Bioelectrochemistry and Bioenergetics*, vol. 43, no. 2, pp. 257-264, 1997.

[34] R. Riener, T. Fuhr, "Patient-driven control of FES-supported standing up: a simulation study," *IEEE Transactions on Rehabilitation Engineering*, vol. 6, no. 2, pp. 113-124, 1998.

[35] R. Riener, J. Quintern, G. Schmidt, "Biomechanical model of the human knee evaluated by neuromuscular stimulation," *Journal of Biomechanics*, vol. 29, no. 9, pp. 1157-1167, 1996.

[36] T. Edrich, R. Riener, J. Quintern, "Analysis of passive elastic joint moment in paraplegics," *IEEE Transactions on Biomedical Engineering*, vol. 47, no. 8, pp. 1058-1065, 2000.

[37] M. Tooley, L. Dingle, *Engineering Science: For Foundation Degree and Higher National*, Routledge, 2013.

[38] B. Ombuki, B. Ross, F. Hanshar, "Multi-objective genetic algorithms for vehicle routing problem with time windows," *Applied Intelligence*, vol. 24, no. 1, pp. 17-30, 2006.

[39] B. Campomanes Álvarez, O. Cordón, S. Damas, "Evolutionary multi-objective optimization for mesh simplification of 3D open models," *Integrated Computer-Aided Engineering*, vol. 20, no. 4, pp. 375-390, 2013.

[40] D. Radu, Y. Besanger, "A multi-objective genetic algorithm approach to optimal allocation of multi-type FACTS devices for power systems security," *IEEE Power Engineering Society General Meeting*, Montreal, QC, Canada, pp. 1-8, 2006.

[41] M. Tapia, C. Coello, "Applications of multi-objective evolutionary algorithms in economics and finance: a survey," *IEEE Congress on Evolutionary Computation*, pp. 532-539, 2007.

[42] C. Fonseca, P. Fleming, "Genetic algorithms for multiobjective optimization: formulation discussion and generalization," *Proceedings of the Fifth International Conference in Genetic Algorithms*, San Mateo, CA: Morgan Kaufmann, pp. 416-423, 1993.

[43] K. Hunt, B. Saunders, C. Perret, H. Berry, D. Allan, N. Donaldson, T. Kakebeeke, "Energetics of paraplegic cycling: a new theoretical framework and efficiency characterisation for untrained subjects," *European journal of applied physiology*, vol. 101, no. 3, pp. 277-285, 2007.

[44] R. Glaser, S. Figoni, S. Hooker, M. Rodgers, B. Ezenwa, A. Suryaprasad, S. Gupta, T. Mathews, "Efficiency of FNS leg cycle ergometry," *Proceedings of the Annual International Engineering in Medicine and Biology Society*, Seattle, WA, USA, pp. 961-963, 1989.